

HIGH LEVELS OF CIRCULARLY POLARIZED EMISSION FROM THE RADIO JET IN NGC 1275 (3C 84)

D. C. HOMAN^{1,2} AND J. F. C. WARDLE³
Accepted for Publication in ApJ Letters

ABSTRACT

We present multi-frequency, high resolution VLBA circular polarization images of the radio source 3C 84 in the center of NGC 1275. Our images reveal a complex distribution of circular polarization in the inner parsec of the radio jet, with local levels exceeding 3% polarization, the highest yet detected with VLBI techniques. The circular polarization changes sign along the jet, making 3C 84 also the first radio jet to show both signs of circular polarization simultaneously. The spectrum and changing sign of the circular polarization indicate that it is unlikely to be purely intrinsic to the emitted synchrotron radiation. The Faraday conversion process makes a significant and perhaps dominant contribution to the circular polarization, and the observed spectrum suggests the conversion process is near saturation. The sign change in the circular polarization along the jet may result from this saturation or may be due to a change in magnetic field order after an apparent bend in the jet. From the small spatial scales probed here, $\simeq 0.15$ pc, and the comparably high levels of circular polarization inferred for the intra-day variable source PKS 1519–273, we suggest a connection between small spatial scales and efficient production of circular polarization.

Subject headings: galaxies : active — galaxies: jets — galaxies: individual: 3C 84, NGC 1275 — polarization

1. INTRODUCTION

Circular polarization from synchrotron emitting radio jets can be a powerful diagnostic of the relativistic fluid transported by the jets. In principle, circular polarization (CP) observations can be used in concert with linear polarization and spectral information to constrain the low energy end of the relativistic particle distribution, measure magnetic field order and strength, and perhaps even deduce the particle content, e^+e^- vs. p^+e^- , of jets (Wardle et al. 1998).

For inhomogeneous synchrotron radiation, circular polarization may be produced as an intrinsic part of the emitted radiation or through the process of Faraday conversion of linear polarization to circular (Jones & O’Dell 1977). On theoretical grounds (e.g. Jones 1988) the Faraday conversion process is expected to dominate over the intrinsic CP of synchrotron radiation in typical jets.

In recent years circular polarization has been detected in a wide range of synchrotron sources: a large number of powerful active galaxies (Wardle et al. 1998; Homan & Wardle 1999; Rayner, Norris, & Sault 2000; Homan, Attridge, & Wardle 2001), low-luminosity AGN such as Sagittarius A* and M81* (Bower, Falcke, & Backer 1999; Sault & Macquart 1999; Brunthaler et al. 2001; Bower, Falcke, & Mellon 2002), intra-day variable sources (Macquart et al. 2000), and galactic microquasars (Fender et al. 2000, 2002). However, the spectral evidence from those objects with constraints at multiple frequencies creates a confusing picture which could be consistent with either intrinsic CP or Faraday conversion (Bower et al. 1999; Sault & Macquart 1999; Macquart et al. 2000; Fender et al. 2000; Brunthaler et al. 2001; Fender et al. 2002). Only in the case of 3C 279 (Wardle et al. 1998) is the Faraday conversion process strongly favored by direct observational evidence.

Here we present multi-frequency Very Long Baseline Array⁴

(VLBA) circular polarization images of the radio source 3C 84 in the center of NGC 1275 ($z = 0.017$). Because of its proximity, we have very high spatial resolution, $\simeq 0.15$ pc, in the radio jet of 3C 84. We report very strong circularly polarized emission in an optically thin region, approximately 0.5 pc south of the peak radio emission. In §2 we describe our observations and calibration techniques. Our results are presented in §3, and we analyze and discuss them in §4.

2. OBSERVATIONS

We observed 3C 84 in December of 1997 (epoch 1997.94) with the VLBA at four frequencies: 5, 8, 15, and 22 GHz. Our nearly full track observations were divided between the observing bands, giving excellent (u,v)-plane coverage and approximately 2 hours on-source per frequency. Here we present and discuss the CP results from our 15 and 22 GHz bands. Total intensity (Stokes I) images are presented in figure 1.

To calibrate the antenna gains to detect circular polarization, we used a modification of the *Zero-V* self-calibration technique described by Homan & Wardle (1999). *Zero-V* self-calibration assumes there is no real circular polarization in the data and calibrates the baseline correlations ($RR = I + V$, $LL = I - V$) versus a pure Stokes I model. The derived antenna gains will act to suppress any real Stokes V in the data; however, except in the case of a point source, the gain “corrections” cannot remove the CP signal completely because the antenna gains are multiplicative while V is additive in the baseline correlations.

For an extended source, like 3C 84, the effect of *Zero-V* self-calibration on real Stokes V will be to reduce its level and induce V of the opposite sign on other strong structure in the source. It is possible to reconstruct the original circular polarization distribution through careful modeling procedures, and that is what we have done. For the 15 and 22 GHz results presented here, the core region is well resolved with a slowly

¹ Karl Jansky Fellow, National Radio Astronomy Observatory, Charlottesville, VA 22903

² Department of Physics and Astronomy, Denison University, Granville, OH 43023; homand@denison.edu

³ Department of Physics, Brandeis University, Waltham, MA; wardle@brandeis.edu

⁴ The VLBA is operated by the National Radio Astronomy Observatory which is a facility of the National Science Foundation operated under cooperative agreement by Associated Universities, Inc.

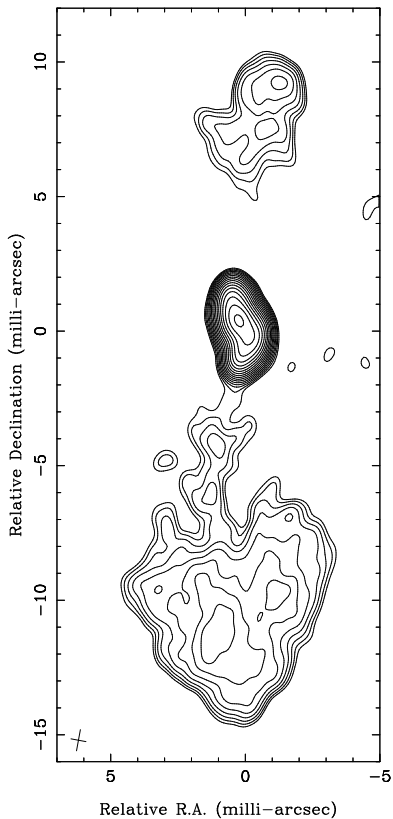


FIG. 1.— VLBA Stokes I images of 3C 84 at 15 GHz. The base contour is 10 mJy/beam, and the contours increase in steps of $\sqrt{2}$. The peaks intensity in the image is 2.79 Jy/beam. The FWHM dimensions of the naturally weighted beam (0.57×0.80 mas \times mas) is depicted by a cross figure in the lower left-hand corner of each panel.

declining brightness profile, so *Zero-V* self-calibration will not greatly distort the real Stokes V (Homan & Wardle 1999); this fact makes the reconstruction process simple and robust.

Figure 2 shows the core region of 3C 84, the distorted CP-signal from *Zero-V* self-calibration, and the reconstruction of the true CP distribution. The reconstruction was done by assuming the peak CP in the distorted map was real, subtracting this CP peak from the original data (prior to self-calibration assuming $V = 0$), calibrating the new subtracted data-set assuming $V = 0$, and examining the resulting residual map. After one iteration, the residual V map still showed signs of real CP which had been distorted by assuming $V = 0$. (We expect this because the original subtraction could not have been large enough. The peak that was subtracted had already been suppressed by some factor in the initial calibration assuming $V = 0$.) So this process was repeated through a number of iterations until the final residual map was flat. We then restored all the subtracted components to the calibrated data.

We ran a large number of tests on this CLEAN-type algorithm⁵ using simulated data, and we found the reconstruction to be robust, particularly for the bright positive components in figure 2. The negative features are real; however, our tests on simulated data showed that the reconstruction algorithm typically reduces their amplitude by $\sim 10\%$ at 15 GHz and $\sim 30\text{--}40\%$ at 22 GHz and may introduce small shifts in their peak position of ~ 0.1 mas. These effects are both due to the weaker nature of negatively polarized components and their closer proximity to the peak of the total intensity structure where the most

distortion will occur from our initial assumption of $V = 0$.

3. RESULTS

Our circular polarization images of 3C 84 are displayed in figures 2 and 3, and we find very strong CP at both 15 and 22 GHz. The registration between the two frequencies was performed on the Stokes I images alone and is illustrated for Stokes V in figure 3. Both the positive and the negative features appear at the same locations at the two frequencies and appear to within a small fraction of a beam-width. All the circularly polarized emission is located south of the map peak, with the change in sign from positive to negative occurring after the jet appears to bend to the east.

The bright knot of positive circular polarization (component “A” in figure 3) is unresolved at 15 GHz and only barely resolved along the jet at 22 GHz. It is located in a part of the jet that has a smoothly declining brightness profile with no distinct features in total intensity. This region of the jet is optically thin with a spectral index of $\alpha = -1$ to -1.5 ($S \propto \nu^{+\alpha}$) for Stokes I between 15 and 22 GHz. The fractional local circular polarization for this spot is $m_c = +3.2 \pm 0.1\%$ at 15 GHz and $m_c = +2.3 \pm 0.2\%$ at 22 GHz. The values are taken at the location of the Stokes V peak, and we can find the spectral index of the fractional circular polarization: $m_c \propto \nu^{-0.9 \pm 0.3}$. Note that the data were weighted and tapered at the two frequencies to give an effectively matched resolution for these measurements.

The negatively polarized components (“B” and “C” in figure 3) are further upstream where the jet is optically thick with $\alpha \simeq +1.2$ at the location of “B” and $\alpha \simeq +1.5$ at the location of “C”. These components have fractional circular polarizations of $m_c = -0.7 \pm 0.1\%$ at 15 GHz and $m_c = -1.3 \pm 0.2\%$ at 22 GHz for component “B” and $m_c = -0.6 \pm 0.1\%$ at 15 GHz and $m_c = -1.0 \pm 0.2\%$ at 22 GHz for component “C”. These values include a $+10\%$ amplitude correction at 15 GHz and a $+30\%$ amplitude correction at 22 GHz to compensate for the typical reductions introduced by our calibration procedure, see §2. The spectral indices of fractional polarization for these negative components are $m_c \propto \nu^{+1.7 \pm 0.6}$ for “B” and $m_c \propto \nu^{+1.4 \pm 0.7}$ for “C”.

It is important to note that our 5 and 8 GHz images (Homan and Wardle, in prep.) show no significant circular polarization in this core region, although a predominantly negative sign of CP is seen farther south in the jet at 5 GHz. The core region is poorly resolved at these longer wavelengths and has become optically thick, so both blending and optical depth may play a role in the lack of detected CP. At the approximate location of component “A”, the Stokes- I spectrum is flat between 8 and 15 GHz and becomes inverted between 5 and 8 GHz, suggesting that the self-absorption turnover for this part of the jet occurs somewhere between 8 and 15 GHz. Assuming $\tau = 1$ at 10 GHz, we estimate the optical depths at 15 GHz and 22 GHz to be $\tau_{15} \sim 0.2$ and $\tau_{22} \sim 0.05$ respectively for component “A”.

No significant linear polarization is detected in the core region at any of our frequencies with an approximate upper limit of 1% at 22 GHz at the location of the strong, positive CP signal analyzed here. The lack of significant linear polarization is most likely explained by external depolarization in a thermal Faraday screen (Wardle 1971) which will have a negligible effect on the circular polarization (Jones & O’Dell 1977; Homan et al. 2001).

⁵ Our procedure differs from a traditional CLEAN-type algorithm in that we improve the calibration with each cycle. We found a loop gain of unity to work well in these cases and tests with a loop gain of one-half showed no significant difference in the results.

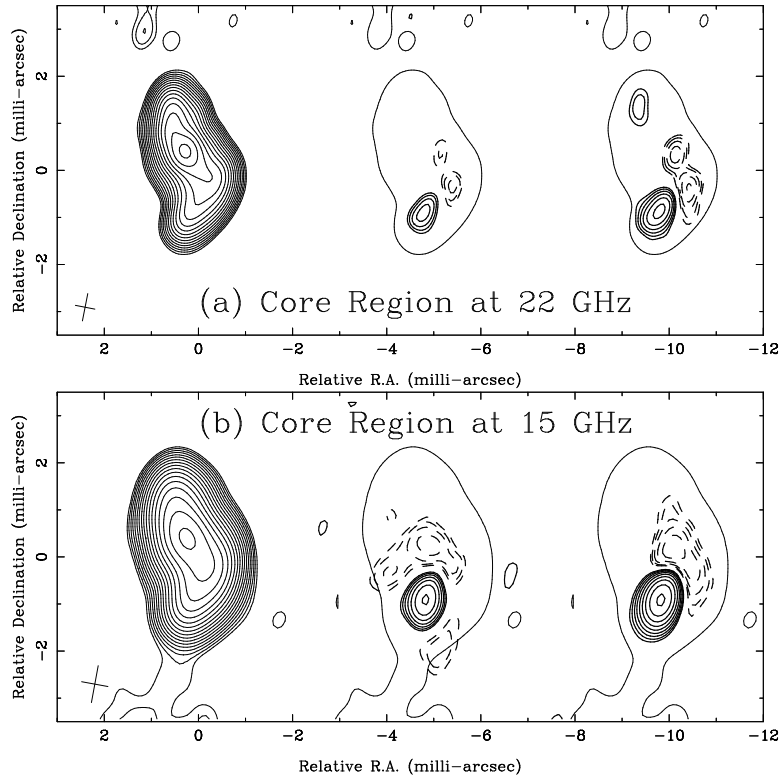


FIG. 1.— Core region of 3C 84 at 22 GHz (a) and 15 GHz (b). *Left*: Stokes I with contours beginning at 10 mJy/beam and increasing in steps of $\sqrt{2}$. *Center*: Stokes V , calibrated assuming $V = 0$, creating some distortion to the true V distribution. *Right*: Stokes V , reconstruction of the true distribution using the algorithm described in §3.1. The V peaks in the reconstructed images are 12.7 mJy/beam at 22 GHz and 33.8 mJy/beam at 15 GHz. For all Stokes- V images the contours begin at 2 mJy/beam and increase in steps of $\sqrt{2}$. A single Stokes I contour is placed around the V images to show registration. The FWHM dimensions of the naturally weighted beams (0.42×0.59 mas \times mas at 22 GHz; 0.57×0.80 mas \times mas at 15 GHz) are depicted by a cross figure in the lower left-hand corner of each panel.

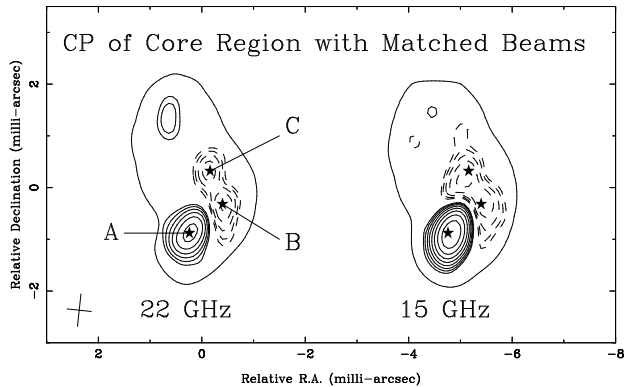


FIG. 3.— Circular polarization of core region of 3C 84 with matched beams at 15 and 22 GHz. The positions of three circularly polarized components are marked in the 22 GHz image. These same positions are indicated in the 15 GHz image to show registration. A single Stokes I contour is placed around the V images to show registration. The common FWHM restoring beam (0.47×0.63 mas \times mas) is depicted by a cross figure in the lower left-hand corner of the image.

4. DISCUSSION AND CONCLUSIONS

We first consider the spot of positive circular polarization which is extremely strong at +3% of the *local* Stokes I at 15 GHz. If the circular polarization is intrinsic to the synchrotron radiation itself, its fractional level varies as $m_c \propto \nu^{-0.5}$ for optically thin emission. This is flatter than our observed spectrum but differs from it by only 1.5σ . The full expression is (Jones & O’Dell 1977; Wardle & Homan 2003)

$$m_c = \epsilon_\alpha^v (\nu_{B_\perp} / \nu)^{0.5} \frac{B_{uu} \cos \theta}{B_\perp^{rms}} \quad (1)$$

where ϵ_α^v is a constant ≈ 2 for $\alpha < -1$ (Jones & O’Dell 1977) and $\nu_{B_\perp} = 2.8 B_\perp^{rms}$ MHz is the gyro-frequency for B_\perp^{rms} in Gauss. $B_{uu} \cos \theta$ is the component of uniform, unidirectional magnetic field along the line of sight responsible for generating the circular polarization. B_\perp^{rms} is the RMS averaged component of field in the plane of the sky and includes contributions not only from the transverse part of B_{uu} but also from disordered field or ordered loops of field which will contribute to Stokes I but not V .

If the circular polarization is entirely due to the intrinsic mechanism, we can estimate the minimum magnetic field strength required by the very high levels of circular polarization detected at 15 GHz. Walker, Romney, & Benson (1994) find the jet of 3C 84 to be only mildly relativistic and oriented at a large angle to the line of sight, $\theta = 30^\circ - 55^\circ$. We take the Doppler factor to be unity and $\theta = 30^\circ$ in these calculations. The largest possible circular polarization will be produced by the intrinsic mechanism when the magnetic field is completely uniform and uni-directional. Under these conditions, $B_\perp^{rms} = B_{uu} \sin \theta$, and we find that a uniform field strength of $B_{uu} \simeq 1$ Gauss is necessary to produce the observed 3.2% circular polarization at $\nu = 15$ GHz. Any sign reversals or disorder in the magnetic field will increase the required magnetic field strength.

Given the above estimate, it is possible that a very strong (~ 1 G), uniform magnetic field along the jet axis is responsi-

ble for generating the observed positive circular polarization via the intrinsic mechanism alone. However, the negative components of circular polarization cannot be easily explained by the intrinsic mechanism. They are located upstream where the jet is optically thick. Pacholczyk & Swihart (1971)⁶ showed that intrinsic circular polarization will change sign when the optical depth is significantly greater than unity, but their results also show that the spectral index of the fractional polarization, m_c , can only be negative after the sign change. This result conflicts with our observations which show a positive spectral index for m_c for both negatively polarized components.

An alternative to a pure intrinsic circular polarization model is to have a significant (and perhaps dominant) contribution from the Faraday conversion effect. High levels of circular polarization can be easily generated via the Faraday conversion process which converts linear polarization to circular (Jones 1988). Faraday conversion operates on Stokes U relative to the local magnetic field orientation (while synchrotron radiation from the same field generates only Stokes Q) and therefore requires either some change in field orientation along the line of sight or some internal Faraday rotation to drive the process. If the conversion process is driven by Faraday rotation, some uniform, unidirectional magnetic field, B_{int} , is required to generate internal Faraday rotation, but here we can have $B_{\text{int}} \ll B_{\perp}^{\text{rms}}$.

In the optically thin regime, the conversion process has a steep spectrum, $m_c \propto \nu^{-3}$, or even steeper if it is driven by Faraday rotation (Wardle & Homan 2003). For the positively polarized, optically thin component, our observed spectrum is flatter than this, $\nu^{-0.9 \pm 0.3}$, and would seem to reject Faraday conversion as the dominant process. However, at $\tau_{15} \sim 0.2$, we are not completely optically thin, and the predicted spectrum flattens as we approach $\tau = 1$ (Jones & O'Dell 1977). This is due to optical depth and saturation in the conversion process as it cycles into a regime where it generates the opposite sign of circular polarization, depolarizing the radiation and flattening the spectrum. This saturation most easily occurs when the conversion process is driven by internal Faraday rotation, as the Faraday rotation will also saturate and begin to depolarize the linear polarization, reducing the amount available for conversion and also flattening the spectrum.

Detailed modeling of this saturation effect is beyond the scope of this paper; however, it is possible to explain not only the spectrum of the positively polarized component but also the change in sign and the spectrum of the negatively polarized components via this mechanism. Of course, the sign change

of polarization from negative to positive may not be due to saturation but rather due to changes in magnetic field order. If the Faraday conversion is driven by Faraday rotation, it is possible to flip the net field polarity and generate the opposite sign of circular polarization. If the Faraday conversion is not driven by Faraday rotation but rather results from a changing field order along the line of sight, as might be the case for a helical field, a change in that field order, such as the pitch angle of the helix, could also change the sign of the resulting circular polarization.

Another interesting aspect of the circular polarization distribution is its apparent break-up into three distinct circularly polarized components while the total intensity (Stokes- I) distribution appears smooth and continuous throughout the region. The sign change of circular polarization between components A and B will naturally make those regions appear separated, since Stokes- V must pass through zero between them. The discrete nature of component C is more difficult to understand. We note that it is closer to the base of the jet and offset from its center, so its discrete appearance may be due to a fortuitous location where the optical depth is not too large and other parameters are suitable for producing significant CP. The magnetic field order in the jet and the presence (or absence) of shocks in the magnetic field may also create enhanced regions of circular polarization; however, without linear polarization information it is impossible to evaluate those possibilities.

Finally, we note that 3C 84, at a redshift of $z = 0.017$, shows the strongest fractional circular polarization yet detected by the VLBA. Much more powerful quasars rarely show local CP stronger than 0.3% (Homan & Wardle 1999; Homan et al. 2001); however, these sources are much farther away and at such distances 3C 84 would have only 0.1–0.2% local circular polarization due to blending with the core. In this light, it is interesting that the intra-day variable source PKS 1519–273 exhibits CP at the 2–4% level in a scintillating component 15–35 μs in size (Macquart et al. 2000). This corresponds to a region of 0.05–0.30 pc in size (for $z \gtrsim 0.2$, Stickel, Fried, & Kuehr 1993), comparable to the linear resolution we achieve in these observations, $\simeq 0.15$ pc. The coincidence of high levels of CP with small spatial scales may be due to the increased relative importance of uni-directional magnetic field (B_{int}) in the jet at small radii (Wardle & Homan 2003).

This work has been supported by the National Radio Astronomy Observatory and by NSF grant AST 99-00723.

REFERENCES

- Bower, G. C., Falcke, H., & Backer, D. C. 1999, *ApJ*, 523, L29
 Bower, G. C., Falcke, H., & Mellon, R. R. 2002, *ApJ*, 578, L103
 Brunthaler, A., Bower, G. C., Falcke, H., & Mellon, R. R. 2001, *ApJ*, 560, L123
 Fender, R., Rayner, D., Norris, R., Sault, R. J., & Pooley, G. 2000, *ApJ*, 530, L29
 Fender, R. P., Rayner, D., McCormick, D. G., Muxlow, T. W. B., Pooley, G. G., Sault, R. J., & Spencer, R. E. 2002, *MNRAS*, 336, 39
 Homan, D. C., Attridge, J. M., & Wardle, J. F. C. 2001, *ApJ*, 556, 113
 Homan, D. C. & Wardle, J. F. C. 1999, *AJ*, 118, 1942
 Homan, D. C. & Wardle, J. F. C. 2000, *ApJ*, 535, 575
 Homan, D. C., & Wardle, J. F. C. 2003, In *Circular Polarization From Relativistic Jet Sources*, a workshop held in Amsterdam, NL, 17-19 July, 2002, eds. R. P. Fender & J.-P. Macquart, *Ap&SS*, 288, 29
 Jones, T. W. 1988, *ApJ*, 332, 678
 Jones, T. W. & O'Dell, S. L. 1977, *ApJ*, 214, 522
 Macquart, J.-P., Kedziora-Chudczar, L., Rayner, D. P., & Jauncey, D. L. 2000, *ApJ*, 538, 623
 Marscher, A. P. 1987, In *Superluminal Radio Sources*, eds. J. A. Zensus & T. J. Pearson (Cambridge: Cambridge Univ. Press), 280
 Pacholczyk, A. G. & Swihart, T. L. 1971, *ApJ*, 170, 405
 Rayner, D. P., Norris, R. P., & Sault, R. J. 2000, *MNRAS*, 319, 484
 Sault, R. J. & Macquart, J.-P. 1999, *ApJ*, 526, L85
 Stickel, M., Fried, J. W., & Kuehr, H. 1993, *A&AS*, 98, 393
 Walker, R. C., Romney, J. D., & Benson, J. M. 1994, *ApJ*, 430, L45
 Wardle, J. F. C. 1971, *Astrophys. Lett.*, 8, 183
 Wardle, J. F. C., & Homan, D. C. 2003, In *Circular Polarization From Relativistic Jet Sources*, a workshop held in Amsterdam, NL, 17-19 July, 2002, eds. R. P. Fender & J.-P. Macquart, *Ap&SS*, 288, 143
 Wardle, J. F. C., Homan, D. C., Ojha, R., & Roberts, D. H. 1998, *Nature*, 395, 457

⁶ The plots given by Jones & O'Dell (1977) consider the combined effects of intrinsic circular polarization and Faraday conversion and here we are interested in the intrinsic mechanism alone. We verified the Pacholczyk & Swihart (1971) result by direct numerical integration of the Jones and O'Dell radiative transfer formulas.